Phenol Removal through Horseradish Peroxidase Immobilization on Ultrafiltration Membranes: Comparative Analysis of Immobilization Methods and Fouling Patterns

Apinya Onsarn, Karnika Ratanapongleka*, Supatpong Mattaraj, Wipada Dechapanya, Tiammanee Rattanaweerapan and Sompop Sanongraj
Department of Chemical Engineering, Faculty of Engineering, Ubon Ratchathani University, Ubonratchathani, Thailand

* Corresponding author. E-mail: karnika.r@ubu.ac.th   DOI: 10.14416/j.asep.2024.07.001

Abstract

This research investigates the removal of phenol using pure peroxidase from horseradish grade I in conjunction with a dead-end ultrafiltration membrane. Various horseradish peroxidase (HRP) immobilization techniques—physical adsorption, covalent bonding, and cross-linking with glutaraldehyde—were applied to a regenerated cellulose (RC) membrane with a surface area of 44 m^2 and a molecular weight cut-off of 30 kDa. The investigation examined factors influencing phenol removal, including phenol concentration, membrane fouling, and the reusability of immobilized enzymes. Results indicated that covalent bonding was the most suitable enzyme immobilization technique, achieving a remarkable 90.1% immobilization yield. Phenol removal efficiency reached 100% at 30 min under specific conditions: phenol concentration of 1 mg/L, pH 6.0, hydrogen peroxide concentration of 0.5 mM, and operating pressure set at 3 psig, with temperature maintained at 28 ± 3 °C. Membrane fouling resulted in a decrease in flux. The performance of fouling models was found to be influenced by phenol concentration, with the Cake Formation Model (CFM) proving most effective at low concentrations, while the Complete Pore Blocking Model (CBM) emerged as more suitable at higher concentrations. The immobilized enzyme exhibited reusability for five cycles, maintaining a phenol removal efficiency exceeding 50%. These findings contribute to understanding the enzymatic phenol removal process and the use of appropriate enzyme immobilization techniques for the effective and sustainable treatment of phenol-contaminated water.

Keywords: Fouling, Horseradish peroxidase, Immobilization, Phenol, Ultrafiltration

1 Introduction

Phenolic compounds, a common group of organic pollutants, are frequently encountered in industrial wastewater effluents, presenting significant environmental and health hazards due to their toxicity and persistence. Among these compounds, phenol is of particular concern owing to its widespread presence in various industrial processes. The alarming levels of phenol found in industries such as petrochemicals (1,345 mg/L), dyes (1,220 mg/L), coal (7,000 mg/L), glass fiber (2,564 mg/L), and resin (1,345 mg/L) underscore the urgent need for effective management strategies [1]. Notably, while phenolic compounds share similarities with other organic pollutants in their impact on the environment and human health, their prevalence and persistence necessitate specific attention. For example, exceeding phenol concentrations of 2 mg/L in natural water sources can lead to adverse effects on aquatic ecosystems and pose risks to human health through contaminated drinking water and recreational activities. Consequently, regulatory bodies like the USEPA classify phenol as a hazardous substance and a carcinogenic compound [2], [3], highlighting the severity of its impact. Given the potential risks associated with phenolic compounds, it is imperative to prioritize research and develop innovative methods for their removal from wastewater. This emphasis

on phenol removal is crucial not only for mitigating immediate environmental and health risks but also for ensuring the long-term sustainability of ecosystems.

Effective methods for phenol removal from wastewater have garnered considerable attention in recent years. Traditional approaches for phenol removal, such as solvent extraction, chemical oxidation, and adsorption on activated carbon [4]–[8], while effective to some extent, often have limitations, including the generation of secondary pollutants and the need for frequent replacement or regeneration of adsorbents. As a result, there is a growing interest in exploring alternative and environmentally friendly approaches for phenol removal, such as enzymatic degradation.

Enzymatic degradation offers several advantages, including high specificity, mild operating conditions, and the potential for enzyme reuse. In this context, horseradish peroxidase (HRP), a heme-containing enzyme, exhibits remarkable detoxification capabilities, versatility across a wide range of pH and temperature conditions, and a notable capacity for phenol removal [9], [10]. It can even operate effectively in acidic conditions, eliminating the need for preliminary treatment steps before introducing substances into the enzymatic removal process [10], [11]. However, there is a limitation when using free enzymes because they cannot be reused. After the treatment process, enzymes are released with the treated water, necessitating continuous enzyme production and extraction for system use, which results in increased enzyme consumption and higher expenses. To efficiently use HRP in wastewater treatment, addressing challenges like enzyme immobilization with membrane technology is crucial.

In recent years, there has been a growing interest in exploring enzyme-immobilized membrane systems for pollutant removal. Studies have delved into the application of enzymes immobilized on membranes, demonstrating their effectiveness. For instance, Yuan *et al*., [12] highlight the potential of fibrous membranes for enzyme immobilization, emphasizing the need for longevity and characterization. Immobilized oxidoreductases on the membrane are highly efficient in converting hazardous organic pollutants such as pharmaceuticals, estrogens, bisphenols, and dyes, with removal rates typically exceeding 90% [13]. Motsa *et al*., [14] investigated laccase-coated polyethersulfone membranes, showcasing their efficiency and reusability

in organic matter degradation and removal. Similarly, Zhu *et al*., [15] focused on laccase-immobilized poly(vinylidene fluoride) membranes, highlighting their versatility and effectiveness in removing azo dyes from wastewater. These studies underscore the potential of enzyme-immobilized membrane systems for industrial wastewater treatment.

The HRP-immobilized ultrafiltration (UF) membrane process for phenol removal involves passing contaminated water through the membrane, where immobilized HRP catalyzes the enzymatic oxidation of phenols, converting them into less harmful substances. Simultaneously, the UF membrane separates purified water from reaction products, offering an eco-friendly, cost-effective solution without the need for chemical reagents. This approach minimizes secondary pollution, reduces enzyme consumption, enables reusability, supports higher loading volumes, and allows for continuous operation [16], [17]. Enzyme immobilization onto UF membranes through chemical methods like covalent attachment and cross-linking typically enhances the enzyme's structural robustness and stability. Nevertheless, predicting how these chemical modifications might affect the enzyme's properties is challenging, as these methods may potentially denature the native enzyme during the binding process. In contrast, physical adsorption is an attractive approach due to its simplicity, cost-effectiveness, and the potential to reuse the membrane once the immobilized enzyme is deactivated [18], [19]. Therefore, it is essential to determine the most suitable method for peroxidase immobilization on UF membranes. However, beyond the immobilization method, significant limitations persist in membrane processes, particularly related to blockages that result in a rapid decrease in flux values. This decline primarily occurs due to concentration polarization, fouling, and the formation of a cake layer on both the membrane's surface and within its pores. These issues inevitably impact the membrane's performance and flux values.

The focus of this work is on the use of horseradish peroxidase (HRP) immobilized on ultrafiltration (UF) membranes as a novel and environmentally friendly approach for phenol removal. The main objectives of the study are: I) to compare different methods of immobilizing the HRP enzyme on a UF membrane, which includes physical adsorption, covalent bonding,

and enzyme cross-linking II) to investigate the efficiency of HRP when immobilized on a UF membrane for removing phenol from contaminated water III) to examine the fouling patterns that occur during the dead-end filtration process.

2 Materials and Methods

2.1 *Enzymes, chemicals and membranes*

Horseradish peroxidase (Grade I), molecular weight 40,000 g/mol, was from AppliChem (Germany), package size 50 KU, enzyme activity 256.4 U/mg (250 Purpurogallin U/mg-solid, more than (RZ > 3.0, salt-free).

The chemicals utilized in this study, including glutaraldehyde, citric acid, hydrogen peroxide, Coomassie Brilliant Blue G250, and Bovine Serum Albumin (BSA) were obtained from AppliChem (Germany). Phenol, 4-aminoantipyrine, guaiacol, and potassium ferricyanide were purchased from Sigma-Aldrich (UK). These chemicals, all of analytical grade, were utilized without the need for additional purification. Deionized water was used in the preparation of the Phenol solution.

The ultrafiltration membrane, manufactured by Millipore Corporation (USA; model number P25594), featured a molecular weight cutoff (MWCO) of 30 kDa. This membrane was constructed from regenerated cellulose, had a cross-sectional area of 44 cm², and was engineered to withstand a maximum pressure of 70 psig (483 kPa). According to the membrane manufacturer's information, the membrane has been verified as suitable for solutions with a pH range of 3.0–13.0, exhibiting chemical resistance, biocompatibility, mechanical strength, and hydrophilic properties.

2.2 *Immobilization methods for HRP on UF membrane*

Three methods of enzyme immobilization (Figure 1) were examined: 1) Physical adsorption, 2) Covalent bonding and 3) Cross-linking. The amount of enzyme introduced to each UF membrane for every method was identical. Each method is described in detail below.

Physical adsorption: After cleaning and pre-compacting a new membrane with deionized water,
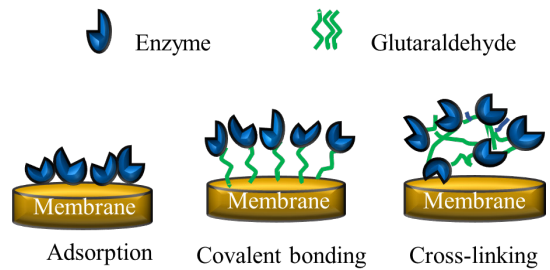

Figure 1: The characteristics of enzyme immobilization through physical adsorption, covalent bonding, and cross-linking methods.

it was immersed in the peroxidase solution for 60 min at a temperature of 4 °C.

Covalent bonding: To initiate activation, the membrane underwent treatment with 0.1% v/v glutaraldehyde for 60 min. After rinsing with deionized water, 0.1 M NaCl, and phosphate buffer, it was then immersed in the peroxidase solution for an additional 60 min at 4 °C. This facilitated enzyme binding to the membrane through amine and aldehyde groups.

Cross-linking: The membrane was first soaked in a solution containing peroxidase and 0.1% v/v glutaraldehyde, then kept at 4 °C for 60 min.

To remove any unbound enzymes after immobilization with each method, the peroxidase-bound membrane was rinsed with deionized water, 0.1 M NaCl, and phosphate buffer under a pressure of 3 psig during operation. This rinsing process was repeated until neither protein nor enzyme activity could be detected in the solution.

2.3 *Dead-end ultrafiltration test cell*

The dead-end ultrafiltration test cell was used to determine the performance of phenol removal by enzymes immobilized on an ultrafiltration membrane. It was pressurized using a nitrogen gas with a purity of 99.5%, which served as the driving force for introducing the substance into the system. The nitrogen gas tank was connected to a stainless-steel sample container with a 10 L capacity, equipped with a pressure gauge capable of measuring up to 100 psig. During operation, the pressure system forces the solution from the sample container through a 400 mL stirred cell module (Amicon 8400, Millipore, USA), housing a single membrane sheet with a diameter of
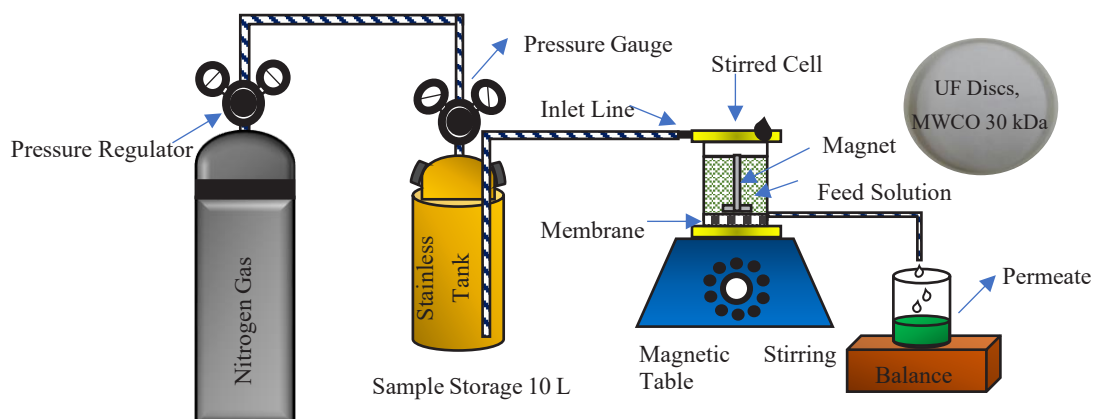
Figure 2: Experimental set-up of a bench-scale stirred dead-end ultrafiltration cell.

7.6 cm and a maximum operating pressure of 75 psig. Inside the stirred cell, a magnetic stirrer propelled the flow at 250 rpm, allowing the permeate to pass through the membrane from the test set into a 500 mL sample collection beaker. The beaker was positioned on an analytical balance (Mettler Toledo PB3002-S) for weight measurement in order to calculate the permeate flux, as shown in Figure 2.

2.4 *Phenol removal experiments*

Three distinct methods of immobilizing HRP on the UF membrane were conducted to assess their performance in removing phenol. These experiments were carried out with a phenol concentration of 1 mg/L and a pH level of 6, in the presence of 0.5 mM hydrogen peroxide. Under operational conditions, the dead-end filtration module was pressurized to 3 psig, and the phenol solution was introduced. The tests proceeded for 240 min. During the experiments, samples were collected from the permeate to analyze residual phenol concentration and assess the enzyme leakage from immobilization. Furthermore, the permeate flux was directly measured, and subsequent normalization was applied to the results. The experiments were consistently conducted in triplicate under stable room temperature conditions.

The most suitable immobilization method, as determined from these tests, was then selected for investigating phenol removal at various concentrations, including 1, 5, 10, and 30 mg/L. These subsequent experiments maintained a pH level of 6, a hydrogen peroxide concentration of 0.5 mm, a system pressure of 3 psig, and a total test duration of 600 min. The results of this experiment were used to analyze the percentage of phenol removal, solution flux, and membrane fouling patterns.

2.5 *Analytical methods*

To evaluate HRP activity, changes in absorbance at 436 nm were measured, employing guaiacol as the substrate and H_2O_2 as the hydrogen source [20]. The substrate mixture, comprising 18 mM guaiacol, 0.05% hydrogen peroxide, and a 0.1 M phosphate buffer pH 7.0, was prepared. In the reaction cuvette, 0.1 mL of the enzyme extract was added to 2.9 mL of the substrate mixture. Enzyme activity was quantified and reported in U/mL.

The absorbance at 510 nm was measured using a UV-VIS spectrophotometer (Shimadzu Corporation, model UV mini1240, Japan) to determine the phenol concentration in the permeate, employing the colorimetric method described previously [21]. Phenol concentrations were derived from the absorbance values by constructing a phenol standard curve.

The Bradford method [22] was employed to determine the protein concentration, based on the colorimetric reaction between proteins and Coomassie Brilliant Blue G250, resulting in a color change. BSA was utilized as the standard protein for developing the calibration curve.

The surface characteristics of the membrane, employing various enzyme immobilization methods,

were examined using a Scanning Electron Microscope (JEOL, JSM-5410LV, Tokyo Japan).

2.6 Reusability of HRP immobilized on the UF membrane

The experiments were conducted in batch mode, involving the repeated utilization of a specified quantity of immobilized enzymes for phenol removal. After each cycle lasting 600 min, the membranes were separated and rinsed with deionized water for 10 min. Subsequently, the reaction solution was replaced with a fresh phenol solution.

2.7 Relevant equations

The percentage of enzyme immobilization can be calculated from the difference between the initial total enzyme activity used for immobilization and the enzyme activity found in the solution and washing solution at the end of immobilization, in comparison to the initial total enzyme activity used for immobilization, as shown in the Equation (1).

$$immobilization\ (\%) = \frac{A_0 - A_t}{A_0} \times 100 \qquad (1)$$

where A_0 is the initial total enzyme activity (U) and A_t is the enzyme activity measured in both the solution and washing solution at the end of immobilization.

The enzyme leakage is measured in terms of the amount of protein found in the permeate compared to the initial quantity of protein introduced into the system. The calculation is shown in Equation (2).

$$Enzyme\ Leakage\ (\%) = \frac{P_t}{P_0} \times 100 \qquad (2)$$

where P_0 is the initial amount of protein introduced into the system (mg) and P_t is the amount of protein detected in the permeate (mg).

Solution flux in membrane filtration can be calculated either by taking membrane permeability and the net transmembrane pressure gradient ($\Delta P - \sigma \Delta \pi$) into account or by dividing the flow rate through the membrane by its cross-sectional area, as shown in Equation (3).

$$J_v = L_p\ (\Delta P - \sigma \Delta \pi) = \frac{Q_p}{A_m} \qquad (3)$$

where J_v represents the solution flux ($Lm^{-2}h^{-1}$, LMH), L_p is the permeation coefficient of the membrane ($LHM\ kPa^{-1}$ or $LMH\ psig^{-1}$), ΔP stands for the pressure driving the system (kPa or psig), σ is the osmotic pressure coefficient, $\Delta \pi$ is the difference in osmotic pressure of the solution at the membrane (kPa or psig), Q_p is the flow rate in the permeate portion (L/h), and A_m is the cross-sectional area of the membrane (m²).

The percentage of phenol removal can be calculated from Equation (4).

$$Phenol\ removal\ (\%) = \left(1 - \frac{C_p}{C_f}\right) \times 100\% \qquad (4)$$

where C_p is the phenol concentration in the permeate and C_f is the phenol concentration in the feed.

The analysis of fouling mechanisms on ultrafiltration membranes uses the Hermia model [23] under constant pressure to explain the decreasing flux mechanism, which can be categorized into four different patterns: Complete Pore Blocking Model (CBM), Intermediate Blocking Model (IBM), Standard Blocking Model (SBM), and Cake Filtration Model (CFM). The linear equations for each model are shown in Table 1, and the fouling mechanisms are depicted in Figure 3.

Table 1: Linear regression equation using Hermia fouling mechanism.

Blocking Mechanism	Linearized Equation Form	Eq.
Complete Pore Blocking Model (CBM)	$ln\ J = ln\ J_0 - K_c\ t$	(5)
Intermediate Blocking Model (IBM)	$1/J = 1/J_0 + K_i\ t$	(6)
Standard Blocking Model (SBM)	$(1/J)^{0.5} = (1/J_0)^{0.5} + K_s\ t$	(7)
Cake Filtration Model (CFM)	$(1/J)^2 = (1/J_0)^2 + K_{cf}\ t$	(8)

when J is the permeate flux (LMH), J_0 is the initial permeate flux (LMH), t is the time (hour), K_c is the constant for Complete pore blocking model fouling, K_i is the constant for Intermediate blocking model fouling, K_s is the constant for Standard blocking model fouling, and K_{cf} is the constant for Cake filtration model fouling, all with units of hour^{-1}.

From Equation (5) to Equation (8), when plotted to analyze the relationship between *ln J* and *t*, 1/J and
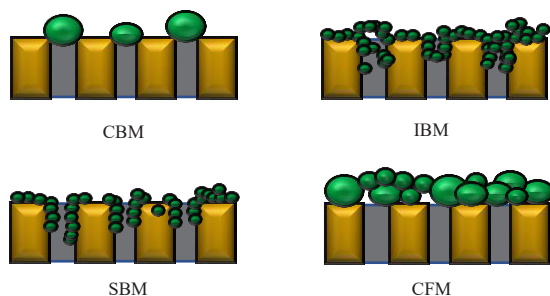
Figure 3: Patterns of fouling mechanisms: Complete Pore Blocking Model (CBM), Intermediate Blocking Model (IBM), Standard Blocking Model (SBM) and Cake Formation Model (CFM).

t, $(1/J)^{0.5}$ and t, and $(1/J)^2$ and t, the values of K_c, K_i, K_s, and K_{cf}, as well as the R^2 value can be determined, by comparing the R^2 values obtained from all four mathematical models, the fouling pattern can be analyzed. If any value approaches 1 the most closely, it can be concluded that the respective model closely resembles the fouling pattern of the membrane. This leads to the conclusion that the membrane exhibits fouling behavior consistent with the best-matching mathematical model.

The mechanisms of the four models can be explained as follows: The Complete Pore Blocking Model (CBM) is characterized by solute molecules reaching the membrane surface, fully blocking the entrance of the pores without entering them, and forming a monomolecular layer on the membrane surface.

The Intermediate Blocking Model (IBM) describes a situation where solute molecules block the flow through the membrane pores. This happens because the additional layer on the membrane's surface can cause solute molecules to adhere to the pores, resulting in reduced flux.

The Standard Blocking Model (SBM) arises from the fact that solute molecules block the flow because they are smaller in size than the membrane pore size, allowing these molecules to penetrate inside the pores.

The Cake Formation Model (CFM) is based on solute molecules accumulating on the membrane surface due to their larger size than the membrane pores, resulting in a cake layer on the membrane surface.
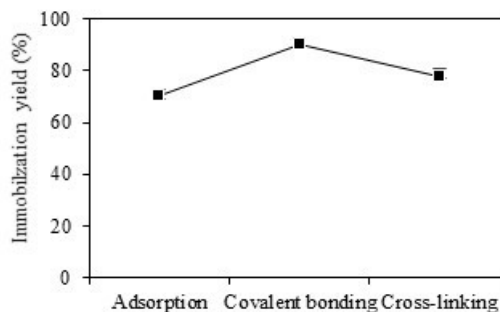

Figure 4: The percentage of immobilization for physical adsorption, covalent bonding, and cross-linking methods.

3 Results and Discussion

3.1 *The effects of enzyme immobilization and enzyme leakage*

The influence of HRP enzyme immobilization on the ultrafiltration membrane is presented in Figure 4, using physical adsorption, covalent bonding, and cross-linking methods. The experimental setup involved an initial enzyme concentration of 0.113 U/cm², a volume of 50 mL, controlled pressure at 3 psig, and a temperature of 28 ± 3 °C. Covalent bonding and cross-linking employed glutaraldehyde as a binding agent, with a concentration of 0.1 (v/v) and an enzyme-to-glutaraldehyde ratio of 1:1. The results showed that covalent bonding achieved the highest immobilization efficiency, reaching 90.1%. In contrast, enzymatic cross-linking and physical adsorption immobilization displayed efficiencies of 78.3% and 70.0% respectively.

Compared to immobilization through physical adsorption and enzyme cross-linking techniques, covalent bonding demonstrated the lowest level of enzyme leakage when considering the percentage of enzyme leakage over an operating period (Figure 5). Within the initial 60 min, enzyme leakage for covalent bonding immobilization was only 1.75%. In contrast, both physical adsorption and cross-linking methods exhibited a continuous release of enzymes. By the end of the 240-minute period, the cumulative enzyme leakage reached 82.3%, 44.5%, and 3.2% for physical adsorption, enzyme cross-linking, and covalent bonding, respectively. Despite HRP having a molecular weight of 40 kDa, which exceeds the molecular cut-off of
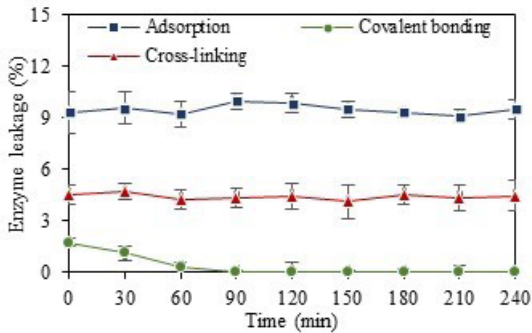
Figure 5: The percentage of enzyme leakage for physical adsorption, covalent bonding, and cross-linking methods.

Figure 6: Scanning electron microscopy images of the membrane surface before use (a), after immobilization through physical adsorption (b), covalent bonding (c), and cross-linking methods (d).

UF membranes, it is still susceptible to leakage, a finding consistent with the research conducted by [16]. The study revealed that the ADH enzyme, with a molecular weight of 141 kDa, surpassing the 50 kDa MWCO of the membrane, also exhibited enzyme leakage. This occurrence could be attributed to the fact that the enzyme consists of a protein tetramer with four identical subunits, each carrying an average molecular weight of around 35 kDa. The relatively low molecular weight of these subunits may explain why the 50 kDa membrane failed to retain the enzyme during extended filtration periods. This explanation can be applied to the similar case of HRP in this study. Additionally, enzyme leakage was observed in the permeate during the immobilization of membranes with lower molecular cut-off values, likely due to the wide range of pore sizes within the membranes. Furthermore, upon the release of pressure, the enzymes seemed to diffuse back into the bulk solution through leakage from the support layer.

The results also indicate that enzyme immobilization by physical adsorption was a process where the enzyme was solely attached to the membrane through ionic bonds and Van der Waals forces, which were relatively weak attractions and lacked chemical bonding. Consequently, this weak interaction made it easier for the immobilized enzymes to detach from the membrane, resulting in a lower immobilization percentage compared to other methods and consistent with the properties of regenerated cellulose (RC) ultrafiltration membranes, which indicate low adsorption properties [24]. On the other hand, covalent bonding and enzymatic cross-linkin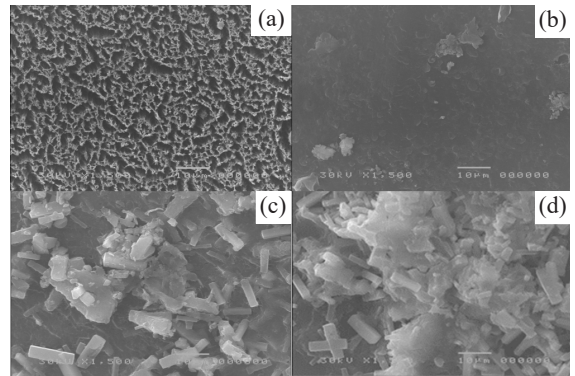g involved chemical bonding through the utilization of reagents, such as glutaraldehyde. In these methods, the enzymes tended to aggregate or agglomerate. This interaction between the enzyme and glutaraldehyde allowed for better adhesion of the enzyme to the membrane surface. The immobilization percentage achieved through covalent bonding was higher compared to the enzyme cross-linking method. This was probably because, during covalent bonding, glutaraldehyde first binds to the membrane, followed by the immobilization of the enzyme, resulting in a complete and strong binding between the enzyme and the binder. In the case of enzyme cross-linking for immobilization, glutaraldehyde was mixed with the enzyme, causing an increase in the enzyme's molecular size. However, this could lead to excessive binding between the enzyme and glutaraldehyde, resulting in overattachment to the enzyme's active site. Consequently, this could deform the enzyme and ultimately reduce its enzymatic function [25].

A study was conducted to analyze the surface characteristics of the ultrafiltration membrane before and after use, utilizing a scanning electron microscope (SEM) at 30 kV with a magnification of 1,500 times. The findings revealed notable observations. Prior to use, as shown in Figure 6(a), the membrane surface displayed numerous distributed pores throughout the sheet. However, after immobilization using physical adsorption (Figure 6(b)), the membrane surface appeared significantly smoother, with some particles retained on the surface. In contrast, covalent bonding immobilization (Figure 6(c)) exhibited densely
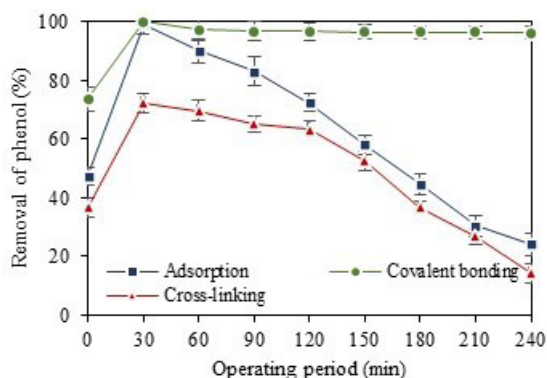
Figure 7: Phenol removal with HRP immobilized on UF membrane.

Figure 8: Solution flux on different immobilization methods.

overlapping particles on the membrane surface. Similarly, the enzyme cross-linking method (Figure 6(d)) demonstrated closely packed particles forming large clusters.

3.2 *The effect of the immobilization method on the removal of phenol and solution flux*

The results of the study on the removal of phenol using HRP immobilized on the ultrafiltration membrane are depicted in Figure 7. The three immobilization methods used were physical adsorption, covalent bonding, and enzyme cross-linking. The experiments were carried out with an initial enzyme concentration of 0.113 U/cm^2, a phenol concentration of 1 mg/L, pH 6, a hydrogen peroxide concentration of 0.5 mM, and a pressure of 3 psig. It was observed that the percentage of phenol removal showed an increasing trend in the initial 30 min of the experiment. The highest phenol removal was achieved within the first 30 min, with removal percentages of 100, 90.2, and 69.6% for the covalent bonding, physical adsorption, and enzyme cross-linking methods, respectively. This indicates that covalent bonding effectively facilitated the attachment of HRP enzymes to the membrane surface, resulting in enhanced phenol removal efficiency. However, as the experiment progressed, the percentage of removal decreased gradually when immobilized by physical adsorption and cross-linking methods. The covalent bonding method proved more effective than other methods, consistently maintaining superior phenol removal throughout the continuous experiment. A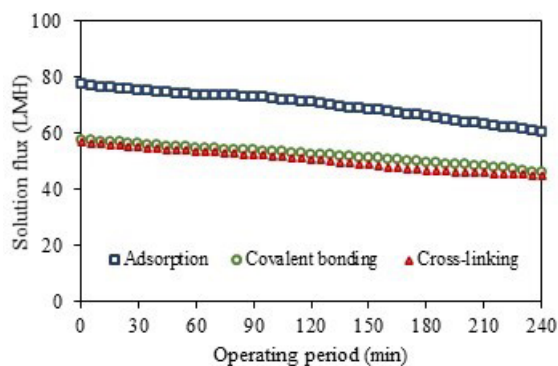dditionally, it has been observed that utilizing covalent bonds is particularly effective for immobilizing α-amylase on cellulose derivative membranes, enhancing reusability and stability compared to immobilization techniques relying on hydrophobic interactions [26]. However, in addition to immobilization methods, the properties of the membrane such as particle size, pore structure, and stability are important for enzyme immobilization [27].

The initial solution flux obtained from the covalent bonding and enzyme cross-linking methods was lower than that obtained from physical adsorption (Figure 8), indicating enhanced stability at the enzyme-membrane interface, thereby leading to consistent membrane performance. As operating time increased, the solution flux gradually decreased across all methods. This decline is attributed to substances becoming trapped on the membrane surface, resulting in their accumulation and increased concentration, causing concentration polarization (CP) and system resistance [28]. Additionally, factors such as substance type, applied pressure, solution pH, and enzyme concentration influence the decrease in flux due to membrane fouling [29].

Overall, the experimental results emphasize the efficacy of covalent bonding in immobilizing HRP enzymes on ultrafiltration membranes for phenol removal. Its ability to achieve high phenol removal percentages and maintain stable membrane performance underscores its potential as a preferred method for enhancing the efficiency and durability of enzyme-immobilized membrane systems. Consequently, this method was chosen for further study.

3.3 *The effect of phenol concentration on removal*

The phenol removal using enzymes immobilized through covalent bonding was examined at various concentrations of phenol, including 1 mg/L, 5 mg/L, 10 mg/L, and 30 mg/L. Throughout the experiment, the pH remained constant at 6, while the hydrogen peroxide concentration was maintained at 0.5 mm. The system operated under a pressure of 3 psig. After 4 h, the removal percentages were as follows: 100%, 65.8, 47.8, and 8.4%, respectively (Figure 9(a)). This phenomenon can be explained by the complete binding of the substrate to the enzyme, which leads to the stabilization of removal efficiency. However, as the concentration of phenol increases, while the immobilized enzyme concentration remains constant, there is a decrease in removal efficiency. This decrease in efficiency may be due to the enzyme not being sufficient to react with the increased phenol concentration. After 10 hours, the removal percentages decreased to 96.5, 56.9, 43.8, and 0% respectively. Furthermore, the products resulting from the HRP-phenol reaction can hinder the enzyme's performance, reducing the efficiency of phenol removal. Moreover, when the phenol concentration is increased, it leads to an accumulation of phenol on the membrane's surface. Over time, this accumulation intensifies, causing phenol to diffuse from areas with higher concentrations to those with lower concentrations. The study's findings are similar to those of [30], which utilized alginate-entrapped turnip peroxidase for phenol removal. They observed that increasing phenol concentration from 20–140 mg/L reduced phenol removal from 30–10%. Furthermore, considering the enzyme leakage (Figure 9(b)) to investigate the correlations leading to the reduced efficiency in phenol removal, it was found that at phenol concentrations of 1, 5, 10, and 30 mg/L, enzyme leakage within the initial 60 min was less than 2%. It can be suggested that the extent of leakage is very minimal and, therefore, has little to no impact on the decreased efficiency in phenol removal or may have only a marginal effect.

The relationship between flux and time in the system is shown in Figure 9(c). It was observed that, at phenol concentrations of 1, 5, 10, and 30 mg/L, there was a clear trend of decreased flux. From the results, it can be explained that as the phenol concentration increases, it leads to a reduction in flux. Furthermore,
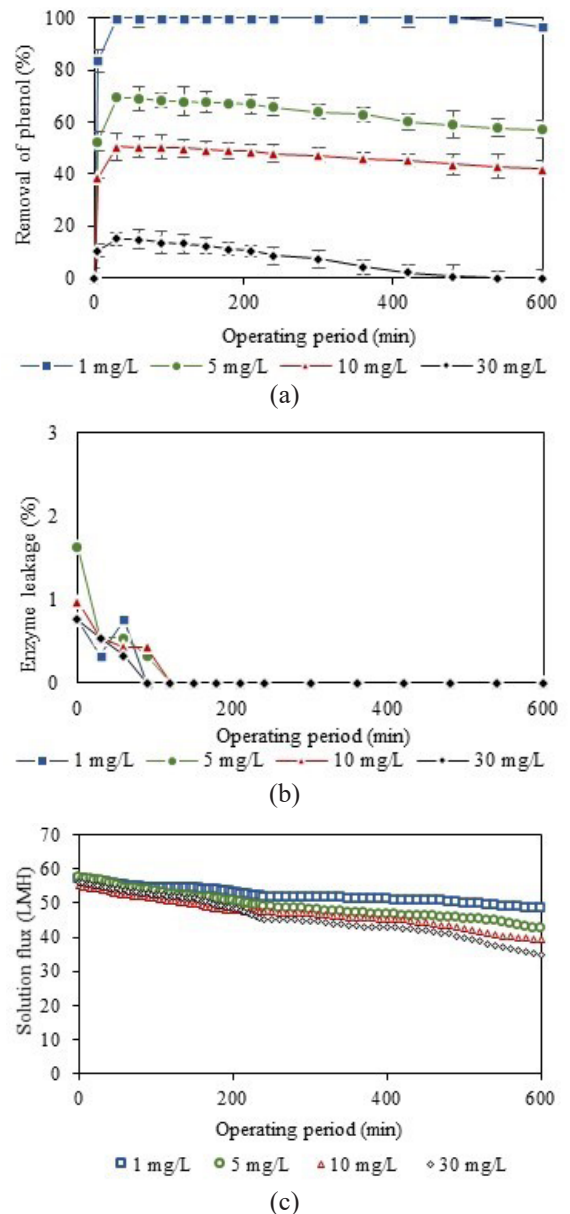

Figure 9: The effect of phenol concentration using HRP immobilized on UF membrane through covalent bonding on the removal (a), enzyme leakage (b), and solution flux (c).

additional investigations revealed that membrane fouling occurs when there is an accumulation of molecules or solute particles that cannot pass through the membrane. With an increase in the system's concentration, accumulation occurs on the membrane surface, and

over time, solute accumulation also increases. This results in the occurrence of concentration polarization (CP) in the system. The development of CP increases the resistance to the flow, causing a reduction in flux.

3.4 *Fouling patterns using the Hermia model*

The permeate flux at each time interval, obtained from experiments conducted under different phenol concentrations, is analyzed using the Hermia mathematical model. This analysis reveals four distinct patterns of membrane fouling: 1) Complete Pore Blocking Model (CBM), characterized by substances or particles perfectly obstructing membrane pores 2) Intermediate Blocking Model (IBM), indicating the presence of substances or particles within the membrane pores 3) Pore Constriction or Standard Blocking Model (SBM), suggesting the blockage of membrane pores by substances or particles and 4) Cake Formation Model (CFM), representing the accumulation of substances or particles on the membrane surface in a layered structure.

Permeate flux data obtained at various phenol concentrations were analyzed using four empirical linear fouling models (refer to Table 1), as depicted in Figure 10. The corresponding regression coefficients for each model are provided in Table 2. The performance of fouling models varies with phenol concentration. At a low phenol concentration of 1 mg/L, the Cake Formation Model (CFM) exhibited the highest R^2 value at 0.971, suggesting that CFM provided the best fit to the experimental data among the considered fouling models. The other models (CBM, IBM, and SBM) also demonstrated good fits but with slightly lower R^2 values. As the phenol concentration increased to 5 mg/L, there was a general improvement in R^2 values for all models. CBM achieved an R^2 of 0.971, IBM reached 0.979, SBM attained 0.976, and CFM demonstrated the highest improvement with an R^2 of 0.984. This suggests that with the increase in phenol concentration, all models performed better, but CFM remained the best fit. The study results are consistent with Luo *et al.*, [18], indicating that the fouling mechanism depends on the membrane material. Regenerated cellulose membranes predominantly experienced cake layer formation due to their hydrophilic nature, facilitating enzyme and solute accumulations and likely forming a cake layer through hydrogen bonding. In contrast,
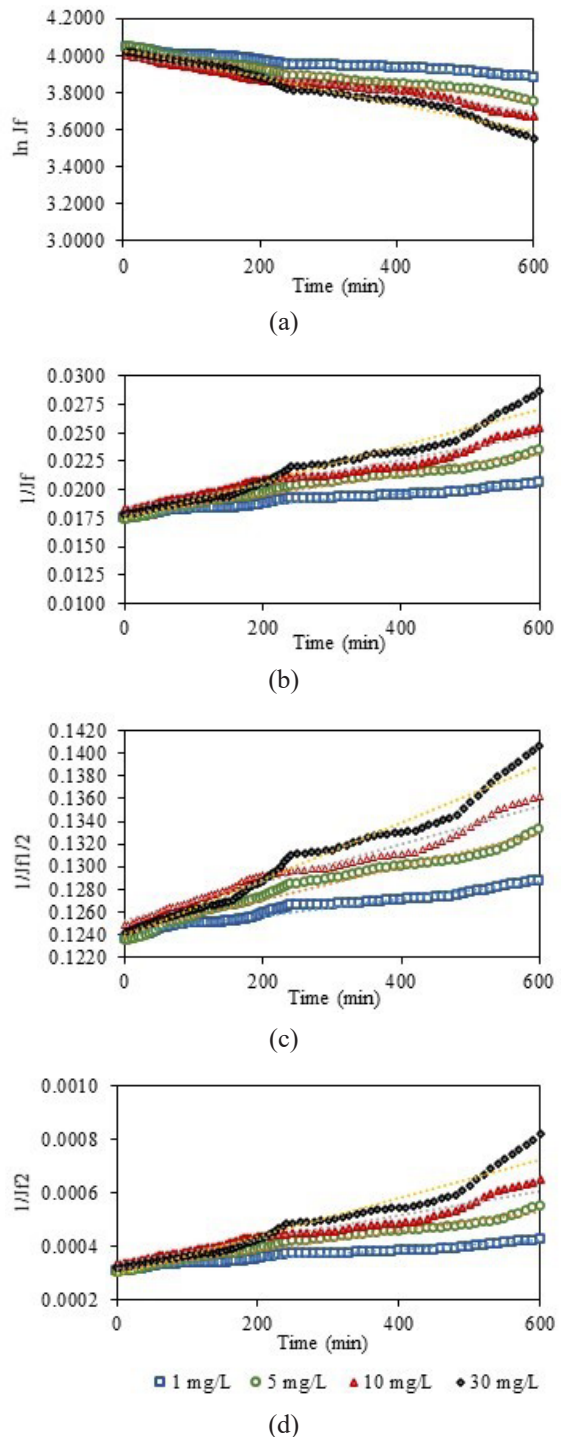

(a)

(b)

(c)

(d)

Figure 10: The fouling mechanism of the membrane using models; (a) CBM, (b) IBM, (c) SBM, and (d) CFM.

polysulphone and polyethersulfone membranes exhibited standard blocking as the principal fouling mechanism, attributed to presumed hydrophobic adsorption. However, at 10 mg/L of phenol concentration, the R^2 values were 0.973 for CBM, 0.970 for IBM, 0.972 for SBM, and 0.961 for CFM.

The decrease in CFM's R^2 value at this concentration indicates a shift in the most effective model, with CBM becoming more suitable for describing fouling patterns. Finally, at the highest phenol concentration of 30 mg/L, CBM maintained the highest R^2 at 0.982, indicating that CBM is the most suitable model for describing fouling patterns at this elevated concentration. The CFM, on the other hand, has a lower R^2 value, suggesting a relatively weaker fit compared to the other models.

Table 2: The comparison of R^2 values obtained from Hermia models describing the fouling patterns of the membrane.

Phenol Concentration (mg/L)	Regression Coefficient, R^2			
	CBM	IBM	SBM	CFM
1	0.963	0.967	0.965	0.971
5	0.971	0.979	0.976	0.984
10	0.973	0.970	0.972	0.961
30	0.982	0.973	0.979	0.955

The transition from CFM at low phenol concentrations to CBM at higher concentrations is a possible occurrence. In situations with low solute concentrations, fouling often involves the formation of a cake layer on the membrane surface, where particles in the feed come together to form a cohesive layer contributing to fouling. This type of fouling is commonly described using the CFM. As the concentration increases, the dynamics of fouling can change. Higher concentrations may lead to increased particle aggregation, particle adhesion to the membrane, or changes in the nature of foulants. This can result in a transition from a cake-dominated fouling mechanism to a more severe fouling mechanism involving pore blocking. At high solute concentrations, the fouling behavior may transition to a CBM, where the membrane pores are progressively blocked by foulants. The increased concentration can accelerate irreversible fouling processes, such as the penetration of solutes into the pores, leading to a decline in permeability and an increase in hydraulic resistance. In addition,

the pore size of the membrane used in this study is larger compared to the size of the phenol molecule. Additionally, the size of the HRP enzyme is similar to the pore size of the membrane. This variability can result in a variety of fouling patterns. Therefore, it is evident that different fouling behaviors can occur in various systems based on factors such as the nature of the enzyme, solute characteristics, membrane properties, and operational conditions. For examples, De Barros *et al.*, [31] determined fouling mechanisms in crossflow UF of enzyme-treated pineapple juice, revealing complete pore blocking for ceramic membranes and cake formation for polymeric membranes. Sokac *et al.*, [32] explored fouling mechanisms in the ultrafiltration of lipase-catalyzed transesterified biodiesel, employing a polyacrylonitrile membrane. The dominant blocking effect was identified as cake formation. Cassano *et al.*, [33] observed the transition from partial to complete pore blocking in crossflow UF of blood orange juice with a tubular PVDF membrane. Marpani *et al.*, [34] discovered the fouling mechanism of alcohol dehydrogenase on an ultrafiltration membrane under different transmembrane pressures (TMP) of 1, 2, and 3 bars. The conclusion states that fouling with standard blocking dominated at 3 bars, while cake formation and intermediate blocking dominated at 1 and 2 bars, respectively. Machado *et al.*, [35] investigated açaí pulp crossflow MF, noting reduced fouling resistance post-enzymatic treatment with dominant cake formation and intermediate/complete pore blocking mechanisms.

3.5 Repeated use of HRP immobilized on a UF membrane

The reusability of immobilized enzymes presents significant advantages, notably cost savings and enhanced method value. By allowing for repeated use without the need for frequent replacements, it reduces procurement costs associated with enzymes and materials. Additionally, reusability enhances the value of the original method by showcasing its durability and reliability over multiple cycles. Reusability without a significant loss in activity is one of the important characteristics of immobilized enzymes. In this study, the ability to reuse HRP immobilized on UF membrane was tested in batch mode, employing identical conditions for all reaction sets. The performance of each repetition
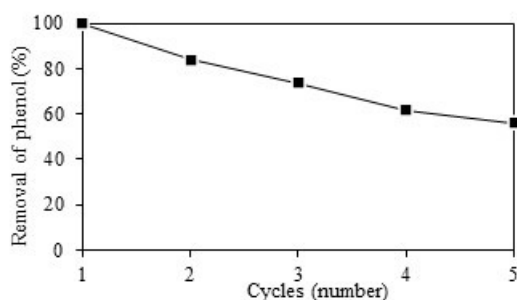
Figure 11: Reuse HRP immobilized on a UF membrane for phenol removal.

was compared to the initial activity, assuming it to be 100%. The results of the study indicate that the phenol removal efficiency for each operational cycle was 100%, 83.9%, 73.7%, 61.9%, and 55.9% for the 1st, 2nd, 3rd, 4th, and 5th cycles, respectively (Figure 11). These findings show the effective reuse of HRP immobilized on the UF membrane for up to five working cycles, with a consistent phenol removal efficiency of over 50%.

Examples of research involving the reuse of enzymes immobilized on a membrane include the application of immobilized peroxidase on a polysulfone UF membrane, effectively decolorizing dye with sustained high activity (70% after reusing three times) [36]. The immobilized laccase on an NF membrane exhibited high catalytic activity and long-term stability in 7 reuse cycles and 36 hours of continuous operation for micropollutant removal [37]. Another study utilized lipase immobilized on a polyacrylonitrile UF membrane, demonstrating successful sustained activity (91.5%) in biodiesel production for six cycles [32]. From these studies, it is evident that reusing immobilized enzymes may impact their efficiency over time. There might be several factors contributing to the gradual decrease in reusability of enzymes immobilized on a UF membrane for this study. One primary reason is enzyme denaturation, often influenced by factors like temperature, pH, and exposure to specific chemicals during filtration cycles. Mechanical stress during filtration processes can contribute to physical damage or alterations in the enzyme's conformation. Accumulation of foulants or by-products on the membrane surface or within the immobilized enzyme layer can hinder active sites, leading to decreased effectiveness. Loss of immobilization integrity, possibly stemming from weak bonding or degradation of the immobilization matrix, may also impact reusability. To improve reusability, the identification of conditions that minimize stress and denaturation is crucial. Additionally, implementing effective cleaning and regeneration protocols for both the immobilized enzyme and the UF membrane can help maintain optimal performance over repeated cycles.

4   Conclusions

The study on phenol removal, using pure peroxidase from horseradish grade I with an ultrafiltration membrane through dead-end filtration, offers significant benefits for the industrial sector and enhances traditional wastewater treatment. Various immobilization techniques for the enzyme on a regenerated cellulose (RC) ultrafiltration membrane were explored, revealing that covalent bonding achieved the highest immobilization efficiency at 90.1%. Optimal conditions for phenol removal were determined, achieving 100% efficiency at 30 min when using a phenol concentration of 1 mg/L, pH 6, hydrogen peroxide concentration of 0.5 mm, an operating pressure of 3 psig, and a temperature of 28 ± 3 °C. The experimental findings provide valuable insights into the effectiveness of using enzymes immobilized through covalent bonding for phenol removal, particularly at a concentration of 1 mg/L. Additionally, the sustained removal efficiency of 96.5% even after 10 hours of operation underscores the longevity and reliability of the enzyme's activity, emphasizing its potential for practical application in wastewater treatment processes. Furthermore, the study's identification of four fouling mechanisms and the demonstration of the immobilized enzyme's reusability for five cycles enhance its practical applicability and sustainability, providing guidance for improving enzyme-based phenol removal processes, enhancing membrane performance, cost-effectiveness, and sustainable treatment.

Author Contributions

A.O.: investigation, data curation and analysis; K.R.: conceptualization, investigation, research design, data analysis, writing an original draft; S.M.: reviewing and editing; W.D.: reviewing and editing; T.R.: reviewing and editing; S.S.: reviewing and editing. All authors have read and agreed to the published version of the manuscript.

Conflicts of Interest

The authors declare no conflict of interest.

References

[1] C. R. Girish and V. R. Murty, "Adsorption of phenol from aqueous solution using Lantana camara, forest waste: Kinetics, isotherm, and thermodynamic studies," *International Scholarly Research Notices*, vol. 2014, 2014, Art. no. 201626.

[2] I. D. Buchanan and J. A. Nicell, "Model development for horseradish peroxidase catalyzed removal of aqueous phenol," *Biotechnology and Bioengineering*, vol. 54, no. 3, pp. 251–261, 1997.

[3] A. T. Nguyen and R.-S. Juang, "Photocatalytic degradation of p-chlorophenol by hybrid H_2O_2 and TiO_2 in aqueous suspensions under UV irradiation," *Journal of Environmental Management*, vol. 147, pp. 271–277, 2015.

[4] A. M. Klibanov, B. Alberti, E. Morris, and L. Felshin, "Enzymatic removal of toxic phenols and anilines from waste waters," *Applied Biochemistry and Biotechnology*, vol. 2, no. 5, 1980, Art. no. 6449569.

[5] M. Djebbar, F. Djafri, M. Bouchekara, and A. Djafri, "Adsorption of phenol on natural clay," *Applied Water Science*, vol. 2, pp. 77–86, 2012.

[6] B. Xie, J. Qin, S. Wang, X. Li, H. Sun, and W. Chen, "Adsorption of phenol on commercial activated carbons: Modelling and interpretation," *International Journal of Environmental Research and Public Health*, vol. 17, no. 3, p. 789, 2020.

[7] J. Liu, J. Xie, Z. Ren, and W. Zhang, "Solvent extraction of phenol with cumene from wastewater," *Desalination and Water Treatment*, vol. 51, no. 19–21, pp. 3826–3831, 2013.

[8] L. G. C. Villegas, N. Mashhadi, M. Chen, D. Mukherjee, K. E. Taylor, and N. Biswas, "A short review of techniques for phenol removal from wastewater," *Current Pollution Reports*, vol. 2, pp. 157–167, 2016.

[9] F. Zhang, B. Zheng, J. Zhang, X. Huang, H. Liu, S. Guo, and J. Zhang, "Horseradish peroxidase immobilized on graphene oxide: Physical properties and applications in phenolic compound removal," *The Journal of Physical Chemistry C*, vol. 114, no. 18, pp. 8469–8473, 2010.

[10] N. C. Veitch, "Horseradish peroxidase: A modern view of a classic enzyme," *Phytochemistry*, vol. 65, no. 3, pp. 249–259, 2004.

[11] J. W. Tams and K. G. Welinder, "Unfolding and refolding of Coprinus cinereus peroxidase at high pH, in urea, and at high temperature. Effect of organic and ionic additives on these processes," *Biochemistry*, vol. 35, no. 23, pp. 7573–7579, 1996.

[12] Y. Yuan, J. Shen, and S. Salmon, "Developing enzyme immobilization with fibrous membranes: Longevity and characterization considerations," *Membranes*, vol. 13, no. 5, p. 532, 2023.

[13] J. Zdarta, K. Jankowska, K. Bachosz, O. Degórska, K. Kaźmierczak, L. N. Nguyen, L. D. Nghiem, and T. Jesionowski, "Enhanced wastewater treatment by immobilized enzymes," *Current Pollution Reports*, vol. 7, pp. 167–179, 2021.

[14] M. Motsa, P. P. Mamba, H. J. Ogola, T. A. Msagati, B. B. Mamba, and T. T. Nkambule, "Laccase-coated polyethersulfone membranes for organic matter degradation and removal," *Journal of Membrane Science and Research*, vol. 8, no. 1, 2022, doi: 10.22079/JMSR.2021.139576.1418.

[15] Y. Zhu, F. Qiu, J. Rong, T. Zhang, K. Mao, and D. Yang, "Covalent laccase immobilization on the surface of poly(vinylidene fluoride) polymer membrane for enhanced biocatalytic removal of dyes pollutants from aqueous environment," *Colloids and Surfaces B: Biointerfaces*, vol. 191, 2020, Art. no. 111025.

[16] I. Alemzadeh and S. Nejati, "Phenols removal by immobilized horseradish peroxidase," *Journal of Hazardous Materials*, vol. 166, no. 2, pp. 1082–1086, 2009.

[17] U. W. Siagian, K. Khoiruddin, A. K. Wardani,

P. T. Aryanti, I. N. Widiasa, G. Qiu, Y. P. Ting, and I. G. Wenten, "High-performance ultrafiltration membrane: Recent progress and its application for wastewater treatment," *Current Pollution Reports*, vol. 7, no. 4, pp. 1–15, 2021.

[18] J. Luo, A. S. Meyer, G. Jonsson, and M. Pinelo, "Enzyme immobilization by fouling in ultrafiltration membranes: Impact of membrane configuration and type on flux behaviour and biocatalytic conversion efficacy," *Biochemical Engineering Journal*, vol. 83, pp. 79–89, 2014.

[19] H.-C. Zhang, S.-X. Gao, and G.-P. Sheng, "Immobilising enzyme-like ligand in the ultrafiltration membrane to remove the micropollutant for the ultrafast water purification," *Journal of Membrane Science*, vol. 636, 2021, Art. no. 119566.

[20] H. Hemeda and B. Klein, "Effects of naturally occurring antioxidants on peroxidase activity of vegetable extracts," *Journal of food Science*, vol. 55, no. 1, pp. 184–185, 1990.

[21] N. Caza, J. Bewtra, N. Biswas, and K. Taylor, "Removal of phenolic compounds from synthetic wastewater using soybean peroxidase," *Water Research*, vol. 33, no. 13, pp. 3012–3018, 1999.

[22] M. M. Bradford, "A rapid and sensitive method for the quantitation of microgram quantities of protein utilizing the principle of protein-dye binding," *Analytical Biochemistry*, vol. 72, no. 1–2, pp. 248–254, 1976.

[23] J. Hermia, "Constant pressure blocking filtration laws – Application to powerlaw non-newtonian fluids," *Transactions of the Institution of Chemical Engineers*, vol. 60, no. 3, pp. 183–187, 1982.

[24] M. Kallioinen, M. Pekkarinen, M. Mänttäri, J. Nuortila-Jokinen, and M. Nyström, "Comparison of the performance of two different regenerated cellulose ultrafiltration membranes at high filtration pressure," *Journal of Membrane Science*, vol. 294, no. 1, pp. 93–102, 2007.

[25] H.-S. Wang, Q.-X. Pan, and G.-X. Wang, "A biosensor based on immobilization of horseradish peroxidase in chitosan matrix cross-linked with glyoxal for amperometric determination of hydrogen peroxide," *Sensors*, vol. 5, no. 4, pp. 266–276, 2005.

[26] N. K. Verma and N. Raghav, "Comparative study of covalent and hydrophobic interactions for α-amylase immobilization on cellulose derivatives," *International Journal of Biological Macromolecules*, vol. 174, pp. 134–143, 2021, doi: 10.1016/j.ijbiomac.2021.01.033.

[27] J. Kujawa, M. Głodek, G. Li, S. I. Al-Gharabli, K. Knozowska, and W. Kujawski, "Highly effective enzymes immobilization on ceramics: Requirements for supports and enzymes," *The Science of the Total Environment*, vol. 801, 2021, Art. no. 149647.

[28] J. W. Chew, J. Kilduff, and G. Belfort, "The behaviour of suspensions and macromolecular solutions in crossflow microfiltration: An update," *Journal of Membrane Science*, vol. 601, 2020, Art. no. 117865.

[29] S.-H. Cho, J. Shim, S.-H. Yun, and S.-H. Moon, "Enzyme-catalyzed conversion of phenol by using immobilized horseradish peroxidase (HRP) in a membraneless electrochemical reactor," *Applied Catalysis A: General*, vol. 337, no. 1, pp. 66–72, 2008.

[30] A. Azizi, M. Abouseoud, and A. Ahmedi, "Phenol removal by soluble and alginate entrapped turnip peroxidase," *Journal of Biochemical Technology*, vol. 5, no. 4, pp. 795–800, 2014.

[31] S. T. D. de Barros, C. M. G. Andrade, E. S. Mendes, and L. Peres, "Study of fouling mechanism in pineapple juice clarification by ultrafiltration," *Journal of Membrane Science*, vol. 215, no. 1, pp. 213–224, 2003.

[32] T. Sokač, M. Gojun, A. J. Tušek, A. Šalić, and B. Zelić, "Purification of biodiesel produced by lipase catalysed transesterification by ultrafiltration: Selection of membranes and analysis of membrane blocking mechanisms," *Renewable Energy*, vol. 159, pp. 642–651, 2020.

[33] A. Cassano, M. Marchio, and E. Drioli, "Clarification of blood orange juice by ultrafiltration: Analyses of operating parameters, membrane fouling and juice quality," *Desalination*, vol. 212, no. 1, pp. 15–27, 2007.

[34] F. Marpani, M. K. Zulkifli, F. H. Ismail, and S. M. Pauzi, "Immobilization of alcohol dehydrogenase in membrane: Fouling mechanism at different transmembrane pressure," *Journal of the Korean Chemical Society*, vol. 63, no. 4, pp. 260–265, 2019.

[35] R. M. D. Machado, R. N. Haneda, B. P. Trevisan,

and S. R. Fontes, "Effect of enzymatic treatment on the cross-flow microfiltration of açaí pulp: Analysis of the fouling and recovery of phytochemicals," *Journal of Food Engineering*, vol. 113, no. 3, pp. 442–452, 2012.

[36] M. Celebi, M. A. Kaya, M. Altikatoglu, and H. Yildirim, "Enzymatic decolorization of anthraquinone and diazo dyes using horseradish peroxidase enzyme immobilized onto various polysulfone supports," *Applied Biochemistry and Biotechnology*, vol. 171, pp. 716–730, 2013.

[37] H. Zhang, J. Luo, J. M. Woodley, and Y. Wan, "Confining the motion of enzymes in nanofiltration membrane for efficient and stable removal of micropollutants," *Chemical Engineering Journal*, vol. 421, 2021, Art. no. 127870.